



The Increased Accumulation of *Staphylococcus aureus* Virulence Factors Is Maximized in a *purR* Mutant by the Increased Production of SarA and Decreased Production of Extracellular Proteases

Duah Alkam,^a Piroon Jenjaroenpun,^b Aura M. Ramirez,^c Karen E. Beenken,^c Horace J. Spencer,^d Mark S. Smeltzer^c

^aDepartment of Biochemistry and Molecular Biology, University of Arkansas for Medical Sciences, Little Rock, Arkansas, USA

^bDepartment of Biomedical Informatics, University of Arkansas for Medical Sciences, Little Rock, Arkansas, USA

^cDepartment of Microbiology and Immunology, University of Arkansas for Medical Sciences, Little Rock, Arkansas, USA

^dDepartment of Biostatistics, University of Arkansas for Medical Sciences, Little Rock, Arkansas, USA

ABSTRACT Mutation of *purR* was previously shown to enhance the virulence of *Staphylococcus aureus* in a murine sepsis model, and this cannot be fully explained by increased expression of genes within the purine biosynthesis pathway. Rather, the increased production of specific *S. aureus* virulence factors, including alpha toxin and the fibronectin-binding proteins, was shown to play an important role. Mutation of *purR* was also shown previously to result in increased abundance of SarA. Here, we demonstrate by transposon sequencing that mutation of *purR* in the USA300 strain LAC increases fitness in a biofilm while mutation of *sarA* has the opposite effect. Therefore, we assessed the impact of *sarA* on reported *purR*-associated phenotypes by characterizing isogenic *purR*, *sarA*, and *sarA/purR* mutants. The results confirmed that mutation of *purR* results in increased abundance of alpha toxin, protein A, the fibronectin-binding proteins, and SarA, decreased production of extracellular proteases, an increased capacity to form a biofilm, and increased virulence in an osteomyelitis model. Mutation of *sarA* had the opposite effects on all of these phenotypes and, other than bacterial burdens in the bone, all of the phenotypes of *sarA/purR* mutants were comparable to those of *sarA* mutants. Limiting the production of extracellular proteases reversed all of the phenotypes of *sarA* mutants and most of those of *sarA/purR* mutants. We conclude that a critical component defining the virulence of a *purR* mutant is the enhanced production of SarA, which limits protease production to an extent that promotes the accumulation of critical *S. aureus* virulence factors.

KEYWORDS *Staphylococcus aureus*, extracellular proteases, osteomyelitis, *purR*, *sarA*

Recent reports have demonstrated that the purine biosynthesis regulator PurR not only represses expression of genes in the purine biosynthesis pathway but also impacts the production of multiple virulence factors in *Staphylococcus aureus* (1). Indeed, mutation of *purR* in a representative isolate of the USA300 clonal lineage was shown to significantly alter the expression of 130 genes, 38 of which were negatively regulated and 92 of which were positively regulated (1). The cumulative result of these changes is increased virulence, as assessed in a murine sepsis model (1–3). Studies examining the impact of mutating genes in the purine biosynthesis pathway confirm that this can be partially attributed to increased *de novo* purine synthesis *in vivo*, but they also demonstrate the involvement of other factors (3). Specifically, *purR* mutants produce increased levels of alpha toxin and the fibronectin-binding proteins FnB A and

Citation Alkam D, Jenjaroenpun P, Ramirez AM, Beenken KE, Spencer HJ, Smeltzer MS. 2021. The increased accumulation of *Staphylococcus aureus* virulence factors is maximized in a *purR* mutant by the increased production of SarA and decreased production of extracellular proteases. *Infect Immun* 89:e00718-20. <https://doi.org/10.1128/IAI.00718-20>.

Editor Nancy E. Freitag, University of Illinois at Chicago

Copyright © 2021 American Society for Microbiology. **All Rights Reserved.**

Address correspondence to Mark S. Smeltzer, smeltzermarks@uams.edu.

Received 10 November 2020

Returned for modification 30 December 2020

Accepted 14 January 2021

Accepted manuscript posted online 19 January 2021

Published 17 March 2021

FnbB, and the increased production of these virulence factors has been shown to contribute to increases in the cytotoxicity for human neutrophils, the invasion of host cells, and overall virulence (1–4). These observations account for the hypothesis that, in addition to its role as a key metabolic regulator of purine biosynthesis, PurR acts as a “moonlighting” protein that modulates the production of critical *S. aureus* virulence factors (1).

Using the *Bacillus subtilis* PurR binding site (5'-AACACCGAACATTA-3') as a guide for *in silico* analysis of the *S. aureus* USA300 FPR3757 genome, a PurR binding site was identified upstream of *fnbA* as well as genes within the purine biosynthesis pathway, and the functionality of these sites was confirmed by demonstrating the binding of PurR to a DNA target corresponding to the respective promoter regions (1). This is consistent with the observation that mutation of *purR* results in increased transcription of *fnbA* and *fnbB* (2). These results suggest that PurR represses expression of these genes directly (1). No PurR binding site was identified upstream of the gene encoding alpha toxin (*hla*), but a binding site was found upstream of the staphylococcal accessory regulator (*sarA*), and SarA was found to be upregulated in a *purR* mutant (1). SarA increases alpha toxin production both directly (5) and indirectly via its ability to increase expression of the accessory gene regulator (*agr*) (6). Based on this and given the lack of a PurR binding site upstream of *hla*, it was suggested that the increased abundance of SarA may account for the increased abundance of alpha toxin and potentially other extracellular proteins (e.g., LukA) in a *purR* mutant (1).

At the same time, the functional status of *sarA* is known to impact the production of extracellular proteases, and changes in the production of these proteases are known to impact the abundance of multiple *S. aureus* virulence factors, including FnbA, FnbB, and alpha toxin (7–11). This raises the possibility that the increased production of SarA may play a role in defining the overall phenotype of *purR* mutants by limiting the production of these proteases, thereby allowing maximum accumulation of *S. aureus* virulence factors, including alpha toxin and the fibronectin-binding proteins. If so, it would be anticipated that mutation of *purR* would result in a reduction in the production of extracellular proteases. There are reports indicating that this is the case (3) but also contradictory reports that *purR* mutants produce increased amounts of almost all of these proteases (1). No PurR binding sites were identified upstream of the genes encoding these proteases, which suggests that, like alpha toxin, any effect of PurR on protease production is likely to occur through an indirect mechanism.

In agreement with the reported moonlighting function of PurR, our transposon sequencing (Tn-Seq) assays in a USA300 (LAC strain) library suggest that the *purR* mutant exhibits increased fitness in a mature biofilm, compared to planktonic cultures; *sarA* mutants, on the other hand, were of decreased fitness in a mature biofilm. Given these observations and the compelling reports described above, we hypothesized that the impact of *purR* on the virulence of *S. aureus* occurs via both direct and indirect mechanisms, the latter being related at least in part to the impact of the mutation of *purR* on the production of SarA (1). To address this possibility, we generated *purR*, *sarA*, and *sarA/purR* mutants in the USA300 *S. aureus* strain LAC. We also generated derivatives of each of these mutants that are unable to produce aureolysin, ScpA, SspA, and SspB. We then characterized all of these mutants with respect to known phenotypes of *S. aureus* *purR* mutants (1, 2), as well as their relative virulence in a murine osteomyelitis model.

RESULTS

Impact of mutating *purR* and *sarA* on fitness in an established biofilm as assessed by Tn-Seq. We have a primary clinical interest in osteomyelitis and other forms of orthopedic infection, and one important factor in defining the therapeutic recalcitrance of such infections is formation of a biofilm (12, 13). With this in mind, we utilized a Tn-Seq library generated in the USA300 *S. aureus* strain LAC (14, 15) to identify mutants that exhibit altered fitness in the context of a mature *in vitro*-grown biofilm. Mutants with mutations in the global regulator *mgrA*, the *ica* operon repressor

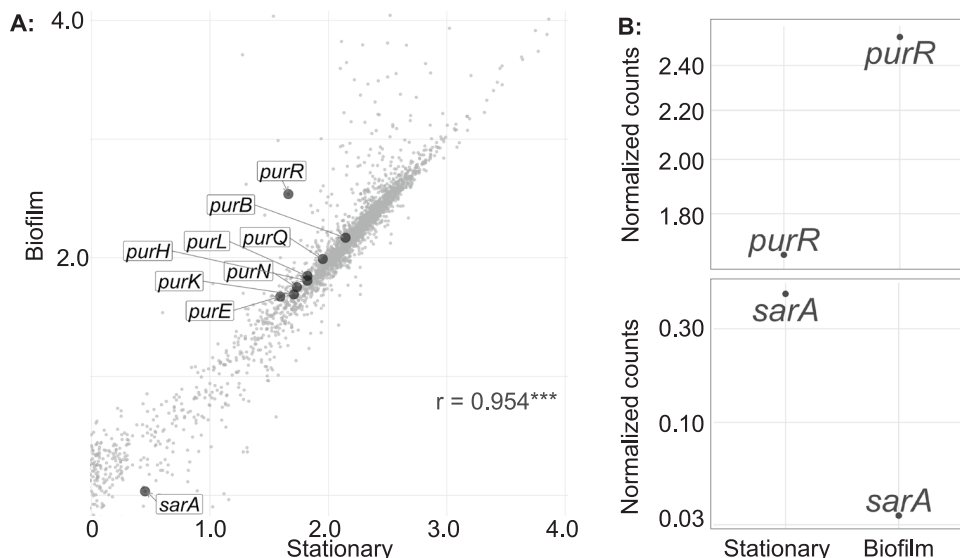


FIG 1 Tn-Seq results related to purine biosynthesis and SarA. A Tn-Seq library generated in the USA300 strain LAC was used to identify mutants with altered fitness in the stationary-growth phase versus a mature biofilm. (A) Pearson's correlation of normalized transposon insertion counts from a mature biofilm versus planktonic culture. *purR*, genes in the purine biosynthesis pathway, and *sarA* are highlighted. ***, $P < 0.001$. Values are presented on a log scale. (B) Inverse relationship between the normalized counts observed with *purR* versus *sarA* mutants in stationary phase versus a biofilm. Values are presented on a log scale.

icaR, and *agrA* and *agrB* were found to be more fit in mature biofilms, compared to planktonic cultures, as evidenced by their increased prevalence in the biofilm-derived library in comparison with the same library grown in planktonic culture (see Table S1 in the supplemental material). This is consistent with previous reports indicating that expression of all of these genes limits biofilm formation (16–20). In contrast, mutants with mutations in other genes implicated in the pathogenesis of *S. aureus* infections were found to exhibit reduced fitness in a biofilm. These genes include *srrB*, which encodes the histidine kinase of the SrrAB two-component signal transduction system shown to be important in a murine osteomyelitis model, and the F_1F_{10} ATPase genes *atpA* and *atpB*, which are part of a pathway previously shown to contribute to virulence in a murine abscess model (Fig. S1) (15, 21).

A list of all mutants that exhibited altered fitness in a biofilm to a statistically significant degree based on a \log_2 fold change of ± 1 is provided in Table S1. This list does not include genes within the purine biosynthesis pathway. However, mutation of *purR* did result in increased fitness in a mature biofilm (Fig. 1A). This was of particular interest to us because mutation of *purR* has been shown to enhance the production of SarA (1). To the extent that mutation of *sarA* limits biofilm formation in diverse clinical isolates of *S. aureus* (22–26), this suggests that the increased fitness of *purR* mutants in a biofilm could be due, at least in part, to increased production of SarA. Indeed, although the reduction in the number of insertions in *sarA* was not statistically significant because of the small number of insertions detected in the planktonically grown comparator, there was an inverse relationship between *purR* and *sarA* in the context of a biofilm (Fig. 1B). We are continuing to investigate the results of our Tn-Seq studies focusing on biofilm formation but, based on these observations, we chose to focus in this report on investigating the significance of *purR* in expression of SarA in defining the accumulation of critical *S. aureus* virulence factors and pathogenesis in the clinical context of osteomyelitis.

Mutation of *purR* results in an increase in the abundance of SarA. A primary factor contributing to the reduced ability of *sarA* mutants to form a biofilm is the increased production of extracellular proteases. With respect to *purR*, the literature is

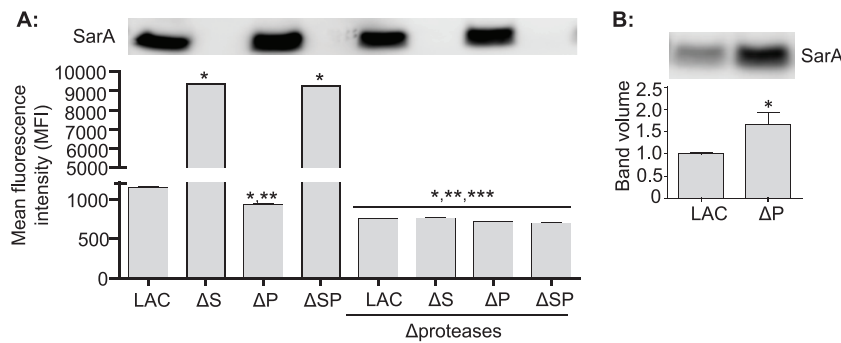


FIG 2 Impact of *purR* and *sarA* on protease production and the production of SarA. Mutations were generated in *sarA* (ΔS), *purR* (ΔP), and both *sarA* and *purR* ($\Delta S P$) in LAC. Additional derivatives in which the genes encoding aureolysin, ScpA, SspA, and SspB were also mutated (Δ proteases) were generated in each of these four strains. (A) Results of Western blots verifying the abundance of SarA and the impact of these mutations on overall protease activity, as determined using a FRET-based assay. *, statistical significance in comparison to the LAC parent strain; **, statistical significance in comparison to the *sarA* mutant; ***, statistical significance in comparison to all strains with the capacity to produce extracellular proteases. (B) Impact of mutating *purR* on the abundance of SarA, as assessed by Western blotting using an anti-SarA antibody. Western blots were performed with anti-SarA antibody and whole-cell lysates prepared from stationary-phase cultures after 1:8 dilution to better illustrate differences in the amount of SarA in LAC versus its isogenic *purR* mutant. The bar chart indicates the combined results from four biological replicates. *, statistical significance in comparison to the results observed with the LAC parent strain. Statistical analysis was performed by ANOVA with Dunnett's correction, with P values of ≤ 0.05 being considered statistically significant.

confusing in this respect, in that there is one report indicating that "secreted proteases have decreased transcription in a *purR* mutant of *S. aureus*" (2), while another found that mutation of *purR* resulted in the increased production of most extracellular proteases (1). Using a gelatin-based fluorescence resonance energy transfer (FRET) assay, we found that mutation of *purR* results in a modest but statistically significant decrease in overall protease activity, while mutation of *sarA* results in a dramatic increase irrespective of the functional status of *purR* (Fig. 2A). We also confirmed that mutation of *purR* results in a significant increase (~2-fold) in the production of SarA (Fig. 2B), thus providing a possible explanation for the observation that mutation of *purR* results in a decrease in overall protease activity.

Mutation of *purR* results in enhanced biofilm formation, increased clumping in the presence of serum, and increased accumulation of specific virulence factors, owing to increased accumulation of SarA and decreased production of extracellular proteases. In agreement with our Tn-Seq results, mutation of *purR* has been reported to result in an increased capacity to form a biofilm (2). The increased production of extracellular proteases plays a key role in limiting biofilm formation in *sarA* mutants (24). This suggests that the limited production of extracellular proteases in a *purR* mutant may be sufficient to enhance biofilm formation, perhaps owing to the increased production of SarA. Reports describing the impact of *S. aureus* mutations on biofilm formation are difficult to put into context, owing to differences in the specific manner by which biofilm formation is assessed. The most commonly used method is a micro-titer plate-based assay, but even then there is considerable variation, most notably in the use of the medium supplements NaCl and/or glucose and whether the substrate is preconditioned by coating with plasma. Our results demonstrate that biofilm formation in *S. aureus* is maximized when the medium is supplemented with both salt and glucose and the substrate is coated with plasma, and these are the standard assay conditions we have employed in all our reports (9, 22–31). In contrast, the previous report demonstrating that mutation of *purR* results in increased biofilm formation did not include NaCl as a supplement or the use of plasma coating (2).

To address this, we assessed biofilm formation under alternative conditions that took all of these factors into account. In every case, tryptic soy broth (TSB) supplemented with glucose was used, with the variables being the inclusion of salt in the

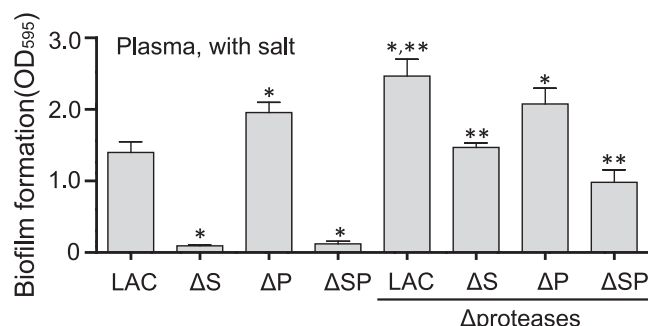


FIG 3 Biofilm formation as a function of *purR*, *sarA*, and extracellular proteases. Biofilm formation was assessed in LAC, its isogenic *sarA* (DS), *purR* (DP), and both *sarA* and *purR* (DSP) mutants, and derivatives of each unable to produce any extracellular protease (Δproteases). All assays used CM from stationary-phase cultures grown in TSB supplemented with glucose. Assays were performed with additional supplementation with NaCl and with human plasma precoating. *, statistical significance in comparison to LAC; **, statistical significance between each strain and its protease-deficient derivative. Statistical analysis was performed by ANOVA with Dunnett's correction, with *P* values of ≤ 0.05 being considered statistically significant.

assay medium and whether the wells of the microtiter plate were preconditioned with human plasma. As in our previous experiments (27), biofilm formation was maximized for the LAC strain under our standard assay conditions (i.e., plasma with salt), and under these conditions mutation of *sarA* resulted in a significant decrease in biofilm formation irrespective of the functional status of *purR*, while mutation of *purR* resulted in an increase in biofilm formation relative to LAC (Fig. 3). With the exception of the *purR* mutant, eliminating protease production significantly enhanced biofilm formation in all strains, including the *sarA/purR* mutant, in comparison to the isogenic mutant capable of producing these proteases. Indeed, this was true even for LAC (Fig. 3). Eliminating protease production did appear to have a greater impact in the *sarA* mutant than in the *sarA/purR* mutant, but in both cases biofilm formation was restored to a degree that was not significantly different from that observed in the LAC parent strain.

The results observed under other assay conditions were similar but not identical. Specifically, in medium supplemented with salt and glucose but in the absence of plasma coating, biofilm formation was reduced in *sarA*, *purR*, and *sarA/purR* mutants in comparison to LAC (Fig. S1A). If salt was not included, then biofilm formation was still reduced in *sarA* and *sarA/purR* mutants, both with (Fig. S1B) and without (Fig. S1C) plasma coating. In contrast, mutation of *purR* resulted in an increased capacity to form a biofilm under both of these conditions, although not to an extent comparable to that observed under our standard assay conditions (Fig. 3). Under test conditions that maximize biofilm formation, there was no significant increase in biofilm formation in a protease-deficient *purR* mutant in comparison to the *purR* mutant itself (Fig. 3). This is perhaps not surprising since, under these test conditions, the *purR* mutant was found to form a robust biofilm, thus making it difficult to reproducibly detect any additional increase. However, under other test conditions in which biofilm formation was not maximized in LAC or its *purR* mutant, an increase was readily apparent in the protease-deficient *purR* mutant (Fig. S1). Taken together, these results are consistent with the hypothesis that the decrease in protease production observed in a LAC *purR* mutant is phenotypically apparent in the context of biofilm formation.

A previous report demonstrated that increased production of the fibronectin-binding proteins FnbA and FnbB plays a key role in defining the hypervirulence of *purR* mutants (2). The increased abundance of these proteins was reflected in the rapid formation, in the presence of horse serum, of visible clumps of bacteria that readily settled out of static cultures, thus resulting in a reduction in the optical density (OD) of the culture. The clumping phenotype in the presence of horse serum was confirmed

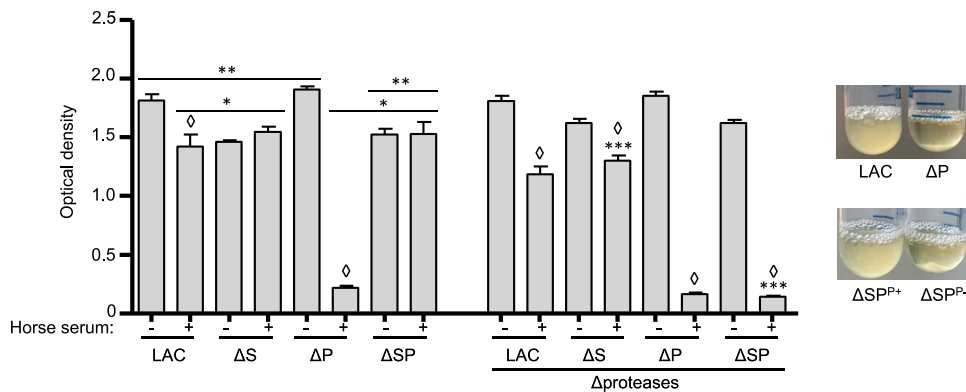


FIG 4 Clumping as a function of *purR*, *sarA*, and extracellular proteases. (Left) Cellular clumping was assessed in LAC, *sarA* (ΔS), *purR* (ΔP), and both *sarA* and *purR* (ΔSP) mutants and the isogenic strains unable to make extracellular proteases (Δ proteases) based on sedimentation of aggregated bacteria after static incubation. Thus, increased clumping is reflected in decreased OD values. *, statistical significance in comparison to LAC; **, statistical significance in comparison to the *purR* mutant in the presence of horse serum. Statistical analysis of data shown on the left was performed by ANOVA with Dunnett's correction. ***, statistical significance of the protease-deficient derivative of each mutant in comparison to the same mutant with the capacity to produce extracellular proteases; \diamond , statistical significance in the presence of horse serum in comparison to the absence of horse serum with the same strain. Statistical comparisons in this case were made by Student's unpaired *t* test. (Right) Visual illustration of the clumping phenotype in LAC, its *purR* (ΔP) mutant, and its isogenic *sarA/purR* mutant (ΔSP) with (ΔSP^+) and without (ΔSP^-) the capacity to produce extracellular proteases.

for the LAC *purR* mutant (Fig. 4). Mutation of *sarA* limits the accumulation of FnbA and FnbB, owing to protease-mediated degradation (7, 9), and it would thus be expected that a *sarA* mutant would not exhibit a clumping phenotype. Mutation of *sarA* limits the growth of *S. aureus* to a modest extent (24) and, under the assay conditions we employed, this was reflected in a slight reduction in OD, relative to LAC, but there was no evidence of a clumping phenotype when the *sarA* mutant was grown in the presence of horse serum. The modest reduction in growth and the absence of a clumping phenotype were also evident in the isogenic *sarA/purR* mutant. Additionally, enhanced clumping in the presence of horse serum was observed in the protease-deficient *sarA* mutant, and the clumping phenotype of the *sarA/purR* mutant was fully restored by eliminating the ability of these mutants to produce extracellular proteases (Fig. 4).

The increased production of alpha toxin has also been implicated in the increased virulence of *purR* mutants (1), and mutation of *sarA* has been shown to limit the accumulation of alpha toxin, owing to protease-mediated degradation (7, 9–11, 29). As assessed by Western blotting, we found that the abundance of alpha toxin was diminished in both *sarA* and *sarA/purR* mutants (Fig. 5A) despite the fact that it was increased in a *purR* mutant (Fig. 5B). The abundance of alpha toxin was also restored in both *sarA* and *sarA/purR* mutants by eliminating their ability to produce extracellular proteases (Fig. 5A). The abundance of protein A was also decreased in *sarA* and *sarA/purR* mutants (Fig. 5A) and increased in the *purR* mutant (Fig. 5B) and, as with alpha toxin, the abundance of protein A was restored in both *sarA* and *sarA/purR* mutants in isogenic derivatives unable to produce extracellular proteases (Fig. 5A).

These results are all based on the analysis of conditioned medium (CM) from stationary-phase cultures grown for 16 h and standardized to an OD of 10.0, and there is evidence to suggest that the impact of *purR* on the accumulation of *S. aureus* virulence factors, specifically alpha toxin, is growth phase dependent (1). To address this, we repeated our alpha toxin and protein A Western blots using CM from exponential-phase cultures. The results confirmed that alpha toxin is decreased in *sarA* and *sarA/purR* mutants and increased in the *purR* mutant, in comparison to the isogenic protease-deficient derivatives of each of these same mutants (Fig. 6). However, they also demonstrated that the abundance of protein A is increased in *sarA* and *sarA/purR*

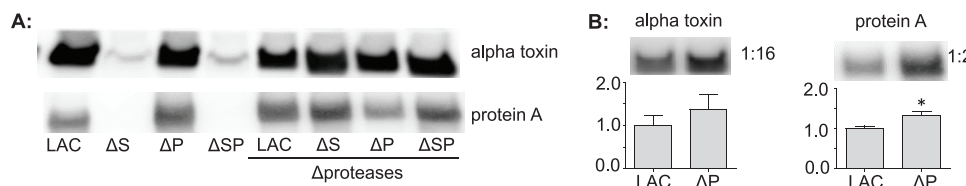


FIG 5 Abundance of alpha toxin and protein A in stationary phase as a function of *purR*, *sarA*, and extracellular proteases. Mutations were generated in *sarA* (ΔS), *purR* (ΔP), and both *sarA* and *purR* (ΔSP) in LAC. Additional derivatives in which the genes encoding aureolysin, ScpA, SspA, and SspB were also mutated (Δ proteases) were generated in each of these four strains. (A) Results of Western blots indicating the relative abundance of alpha toxin (top) and protein A (bottom) in each strain. (B) Impact of mutating *purR* on the abundance of each of these proteins as assessed by Western blotting. Western blots were performed with anti-alpha toxin or anti-protein A antibodies using CM from stationary-phase cultures. (B) CM was diluted by the indicated factor prior to blotting to better illustrate differences in the amount of each protein in LAC versus its isogenic *purR* mutant. The bar chart indicates the combined results from three biological replicates. *, statistical significance ($P \leq 0.05$) in comparison to LAC, as determined using Student's *t* test.

mutants when assessed using CM from exponential-phase cultures. In contrast, the abundance of protein A was unaffected in the isogenic *purR* mutant (Fig. 6).

Overall, the results we report suggest that the increased production of SarA observed in a LAC *purR* mutant plays an important role in defining the *in vitro* phenotypes of *purR* mutants and does so owing to the impact of *sarA* on the production of extracellular proteases. However, the significance of this is called into question by the growth-phase-dependent results observed with respect to the abundance of protein A. No such differences were observed with respect to the fibronectin-binding proteins and alpha toxin, and these are the virulence factors that have been most directly implicated in the hypervirulence of *purR* mutants in a murine sepsis model (1–4). Nevertheless, our clinical focus is on the pathogenesis and therapeutic recalcitrance of osteomyelitis, and protein A has been implicated as an important virulence factor in this clinical context (32–35). To the extent that the exponential- and stationary-growth phases are defined by *in vitro* growth conditions that cannot be definitively correlated with growth *in vivo*, this makes it important to assess the relevance of our results *in vivo* in the context of osteomyelitis.

Additionally, mutation of genes within the purine biosynthesis pathway (e.g., *purB*) attenuates virulence in a murine osteomyelitis model (36), and we have shown that mutation of *sarA* also limits virulence in this model, owing in large part to the increased production of extracellular proteases (9, 29, 31). Moreover, in a previous study we examined the relative impact of *sarA* and *saerS* on virulence in our osteomyelitis model, and this allowed us to identify isogenic mutants that exhibited significant differences in virulence depending on the functional status of these two regulatory loci (9). Proteomic comparisons of these strains showed that FnbA and FnbB were present in much larger amounts (log₂ fold changes of ≥ 5) in virulent strains (9). Thus, the

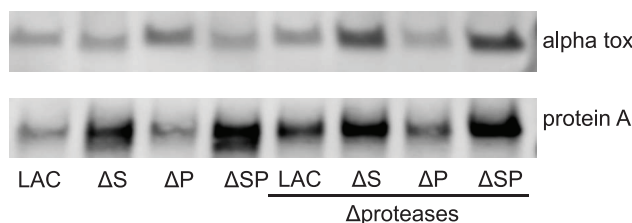


FIG 6 Abundance of alpha toxin and protein A in exponential phase as a function of *purR*, *sarA*, and extracellular proteases. Mutations were generated in *sarA* (ΔS), *purR* (ΔP), and both *sarA* and *purR* (ΔSP) in LAC. Additional derivatives in which the genes encoding aureolysin, ScpA, SspA, and SspB were also mutated (Δ proteases) were generated in each of these four strains. Results shown are representative Western blots indicating the relative abundance of alpha toxin (top) and protein A (bottom) in each strain during the exponential-growth phase.

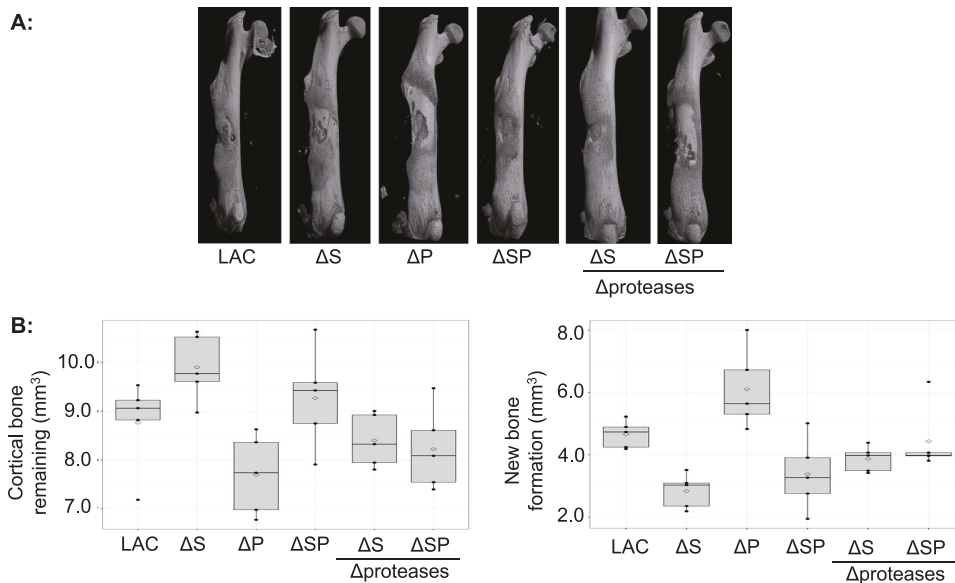


FIG 7 Impact of mutating *purR* and *sarA* and the production of extracellular proteases on virulence in a murine osteomyelitis model. (A) μCT images from mice infected with LAC, *sarA* (ΔS), *purR* (ΔP), and both *sarA* and *purR* (ΔSP) mutants and the isogenic strains unable to make extracellular proteases (Aproteases) were taken 14 days after initiation of the infection. Images shown are from the single mouse from each group that exhibited scores that most closely approximated the median observed for each experimental group. (B) Results of quantitative analysis of μCT images from all mice in each experimental group based on cortical bone destruction (left) and reactive new bone (callous) formation (right). Results are shown as box plots reflecting values derived from groups of five mice each infected with the noted strain. Statistical significance analyses are detailed in Table S2 in the supplemental material.

fact that the abundance of FnbA and that of FnbB are inversely affected by mutation of *purR* versus *sarA* further emphasizes the need to assess the relevance of our results in the clinical context of osteomyelitis.

***purR* mutants are hypervirulent in murine osteomyelitis in a manner dependent on SarA and extracellular proteases.** Our *in vivo* studies were limited to LAC, its isogenic *sarA*, *purR*, and *sarA/purR* mutants, and isogenic *sarA* and *sarA/purR* mutants unable to produce any extracellular protease other than those encoded within the *spl* operon. The results confirmed that mutation of *sarA* limited virulence, as evidenced by both reduced cortical bone destruction and decreased reactive bone formation (Fig. 7 and Table S2). In contrast, the *purR* mutant exhibited a significant increase in cortical bone destruction and new bone formation, compared to LAC. In line with our *in vitro* assays, the virulence phenotype of the *sarA/purR* mutant was comparable to that of the isogenic *sarA* mutant and significantly different from that observed with the isogenic *purR* mutant. As assessed by cortical bone destruction, virulence was restored in both the *sarA* and *sarA/purR* mutants by eliminating the capacity of these mutants to produce aureolysin, ScpA, SspA, and SspB (Fig. 7 and Table S2). Eliminating the production of these proteases also resulted in an increase in new bone formation in comparison to the *sarA* and *sarA/purR* mutants, although in this case the increase was not found to be statistically significant (Fig. 7 and Table S2). Bacterial burdens in the bone were significantly reduced in *sarA* and *sarA/purR* mutants, compared to LAC, but not in the isogenic *purR* mutant (Fig. 8 and Table S2). Moreover, unlike the other phenotypes examined, the phenotype of the *sarA/purR* mutant was more similar to that of the *purR* mutant than to that of the isogenic *sarA* mutant. Eliminating the production of aureolysin, ScpA, SspA, and SspB also resulted in a significant increase in bacterial burden in the bone in the *sarA* mutant (Fig. 8 and Table S2).

DISCUSSION

PurR has been shown to provide a critical link between central metabolism and

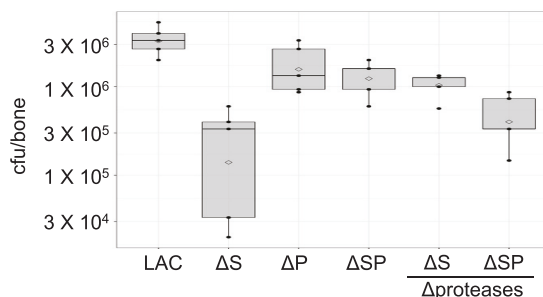


FIG 8 Impact of mutating *purR* and *sarA* and the production of extracellular proteases on bacterial burdens in the bone. Mice were infected with LAC, *sarA* (ΔS), *purR* (ΔP), and both *sarA* and *purR* (ΔSP) mutants and the isogenic strains unable to make extracellular proteases (Δ proteases). All of the *in vitro* data indicate that *sarA* is epistatic to *purR*, but this indicates the opposite. CFU values are presented on a log scale. Results are shown as box plots reflecting values derived from groups of five mice each infected with the noted strain. Statistical significance analyses are detailed in Table S2 in the supplemental material.

virulence in *S. aureus*, owing to its ability to directly regulate expression of genes within the purine biosynthesis pathway and independently regulate genes encoding critical virulence factors, including the fibronectin-binding proteins and alpha toxin (1–4). Indeed, mutation of *purR* in the USA300 strain LAC was shown to result in increased or decreased expression of 130 genes (1). The data available to date suggest that some of these genes are regulated directly via PurR binding to a conserved binding site, while others are regulated indirectly (1, 2). In the case of genes within the purine biosynthesis pathway and the fibronectin-binding proteins, regulation appears to be direct, with PurR acting as a repressor. This presumably ensures that expression of the genes required for purine biosynthesis is limited under conditions in which purines are readily available and that production of virulence factors like the fibronectin-binding proteins is limited to conditions in which they are needed to promote other factors, including but likely not limited to colonization, biofilm formation, and potentially internalization by host cells (2, 37–39). Mutation of *purR* has also been shown to result in the increased production of alpha toxin, but this appears to occur via an indirect mechanism, since no PurR binding site has been found upstream of the *hla* gene encoding alpha toxin (1). In a previous report, this was attributed to increased expression of the staphylococcal accessory regulator (*sarA*), which does contain a putative PurR binding site and is known to positively regulate expression of *hla* both directly and indirectly by enhancing expression of the accessory gene regulator (*agr*). The impact of *sarA* on expression of *agr* could presumably also account for why most *S. aureus* extracellular proteases were found to be present in increased amounts in a *purR* mutant (1). However, there is also a report suggesting that mutation of *purR* results in decreased transcription of the genes encoding extracellular proteases (3), which is consistent with the results we report demonstrating the decreased abundance of these proteases in a LAC *purR* mutant.

These observations account for the underlying hypothesis behind the experiments we report. Additionally, our Tn-Seq assays revealed that the *purR* mutant exhibits increased fitness in a mature biofilm, compared to planktonic stationary-phase cells grown in the same medium. In contrast, none of the mutations in genes involved in the *de novo* purine biosynthesis pathway was found to impact fitness in a biofilm, perhaps owing to the continual replacement of the medium in our flow cells. These findings are consistent with the hypothesis that PurR serves regulatory roles beyond its impact on purine biosynthesis (1, 2). This led us to investigate the role of PurR in regulating the production of SarA. Specifically, much of our focus in recent years has been on *sarA*, owing to the fact that mutation of *sarA* results in a greater decrease in the ability to form a biofilm than mutation of any other regulatory loci we have examined

(9, 22, 24–31, 40). We have also confirmed that this can be directly correlated with the increased production of all extracellular proteases and this results in the reduced accumulation of multiple *S. aureus* virulence factors and reduced virulence in murine models of sepsis and osteomyelitis (7, 9–11, 29, 31). Included among the virulence factors that are present in reduced amounts in *sarA* mutants as a result of protease-mediated degradation are alpha toxin and the fibronectin-binding proteins. Given that mutation of *purR* results in increased production of SarA, this suggests that the increased accumulation of these virulence factors in *purR* mutants may be at least partly attributable to the increased production of SarA, which would presumably limit protease production and maximize the abundance of these virulence factors at times when they are needed most.

To test this hypothesis, we generated *sarA*, *purR*, and *sarA/purR* mutants in the USA300 strain LAC. We also generated isogenic derivatives of all of these mutants that are unable to produce the extracellular proteases aureolysin, ScpA, SspA, and SspB. We then evaluated the impact of these mutations on phenotypes previously implicated in the hypervirulence of *purR* mutants and the relative virulence of these mutants in a murine osteomyelitis model. The results confirmed that mutation of *sarA* results in an increase in overall protease activity while mutation of *purR* has the opposite effect. They also confirmed that protease production was increased in the *sarA/purR* mutant to a level comparable to that observed in the isogenic *sarA* mutant. This would be anticipated if the impact of PurR on protease production were mediated through its impact on the production of SarA, particularly since no PurR binding sites have been identified upstream of the genes encoding any of the targeted extracellular proteases (1).

The impact of these mutations on biofilm formation was somewhat dependent on the assay conditions used, but the inverse relationship between *purR* and *sarA* with respect to protease production and the epistatic impact of *sarA* in a *sarA/purR* mutant were also evident in this regard. Specifically, biofilm formation was increased in the LAC *purR* mutant and decreased in the isogenic *sarA* and *sarA/purR* mutants. Under all experimental conditions examined, biofilm formation was enhanced in all mutants and in LAC itself when the ability to produce aureolysin, ScpA, SspA, and SspB was eliminated by mutation of the corresponding genes. This confirms that protease production limits biofilm formation, particularly in a *sarA* mutant, and that this is true irrespective of the functional status of *purR*.

Although mutation of *purR* alters the expression of multiple genes encoding *S. aureus* virulence factors, there is compelling evidence that the increased production of the fibronectin-binding proteins FnbA and FnbB plays a key role in defining the increased virulence of a *purR* mutant in a murine sepsis model (2). A phenotypic marker proven to reflect the increased production of these surface-associated proteins is increased clumping in the presence of horse serum. This phenotype was clearly evident in the LAC *purR* mutant and absent in the isogenic *sarA* mutant. This is consistent with the observation that mutation of *purR* results in an increase in production of the fibronectin-binding proteins, while these proteins are present in limited amounts in *sarA* mutants as a result of protease-mediated degradation (26). As with protease production and biofilm formation, concomitant mutation of *sarA* abolished the clumping phenotype of the *purR* mutant. The fact that this was also due to the increased production of extracellular proteases in the *sarA/purR* mutant was confirmed by demonstrating that the clumping phenotype of the *sarA/purR* mutant was fully restored by simultaneously eliminating the production of aureolysin, ScpA, SspA, and SspB. Similarly, protein A was also present in an increased amount in a LAC *purR* mutant and was virtually absent in *sarA* and *sarA/purR* mutants at stationary phase, and this phenotype was reversed by eliminating the production of these same proteases.

It has been demonstrated that alpha toxin is produced in elevated amounts in a *purR* mutant and that this also contributes to its increased virulence (1). As with the fibronectin-binding proteins and protein A, we confirmed that the amount of alpha

toxin is increased in a *purR* mutant and decreased in *sarA* and *sarA/purR* mutants. Also, as with these other proteins, the reduced accumulation of alpha toxin was reversed in *sarA* and *sarA/purR* mutants unable to produce key extracellular proteases. To the extent that *agr* enhances the production of alpha toxin and represses the production of the fibronectin-binding proteins and protein A, the fact that the results we observed with all of the proteins were consistent suggests that the impact of mutating *sarA* on these phenotypes is independent of *agr*. Thus, to the extent that the impact of *sarA* on protease production has been shown to be independent of its impact on expression of *agr* (24), all of these results are consistent with the hypothesis that the increased production of important virulence factors that contribute to the hypervirulence of *purR* mutants is dependent, at least in part, on the increased production of SarA and the resulting decrease in the production of extracellular proteases that would otherwise limit the accumulation of these virulence factors. Indeed, the importance of this presumably accounts for the presence of a PurR binding site upstream of the gene encoding SarA (1).

Finally, to assess the *in vivo* relevance of these observations, we evaluated the relative virulence of LAC, its *sarA*, *purR*, and *sarA/purR* mutants, and derivatives of each unable to produce aureolysin, ScpA, SspA, and SspB in a murine osteomyelitis model. The results confirmed our previous reports demonstrating that mutation of *sarA* limits virulence in this model and that virulence is restored to a significant degree by eliminating the ability of a *sarA* mutant to produce extracellular proteases (9). These previous experiments were performed with a LAC *sarA* mutant unable to produce any extracellular protease, including the *spl*-encoded proteases, while the studies we report here utilized protease-deficient mutants that retained the capacity to produce the *spl*-encoded proteases. This suggests that the *spl*-encoded proteases play little role in defining the phenotype of *sarA* mutants, in comparison to aureolysin, ScpA, SspA, and SspB, but this remains to be examined in a more direct and definitive manner.

In contrast to *sarA*, mutation of *purR* significantly enhanced virulence in our osteomyelitis model, as it was previously shown to do in a murine sepsis model (1, 2). This is important because it indicates that *purR* plays an important role in both acute and chronic forms of *S. aureus* infection. The possibility that this is due to increased expression of the genes within the purine biosynthesis pathway cannot be ruled out, particularly since mutation of the genes within this pathway has been shown to attenuate virulence in both of these models (1, 36). However, in comparison to the *purR* mutant, we also demonstrate that virulence is attenuated in the *sarA/purR* mutant and, to our knowledge, *sarA* is not known to play a role in the regulation of purine biosynthesis. The fact that bacterial burdens in the bone were higher in the *purR* mutant than in the *sarA* mutant is consistent with the observation that the *purR* mutant exhibited increased virulence while the opposite was true for the *sarA* mutant. However, in contrast to every other phenotype we assessed, bacterial burdens observed with the *sarA/purR* mutant were more similar to those observed with the *purR* mutant than to those observed with the isogenic *sarA* mutant. This suggests that, with respect to survival *in vivo*, mutation of *purR* may play a more predominant role than mutation of *sarA*, owing to its impact on purine biosynthesis, while in the context of virulence the opposite is true, owing to the increased production of extracellular proteases and its impact on the abundance of important *S. aureus* virulence factors, including alpha toxin and the fibronectin-binding proteins. To the extent that the increased virulence of a *purR* mutant was not correlated with an increase in bacterial burdens in the bone, in comparison to the LAC parent strain, this provides an indication of the important moonlighting functions of PurR on virulence.

Thus, we propose a model in which the impact of mutating *purR* on the virulence of *S. aureus*, at least in the methicillin-resistant USA300 strain LAC, is dependent to a significant extent on the ability of PurR to repress the production of SarA. With respect to *sarA*, such a model reflects the need to limit the production of extracellular proteases such that they serve their intended roles in tissue invasion, avoiding host defenses,

and the acquisition of nutrients without compromising the availability of critical virulence factors (7, 9, 41, 42). In the case of *purR*, its metabolic and moonlighting functions would limit expression of genes in the purine biosynthesis pathway and the production of many of these same virulence factors based on need in specific *in vivo* microenvironments and under changing conditions within the host. Under adverse conditions in which nutrients are limited and biofilm formation potentially offers a survival advantage, reduced production of PurR would both promote purine biosynthesis and maximize the accumulation of critical virulence factors both directly and indirectly by increasing the production of SarA and consequently limiting the production of extracellular proteases, thus maximizing the abundance of important virulence factors.

Finally, the increasing prevalence of antibiotic resistance in *S. aureus* emphasizes the need to consider alternative therapeutic strategies, including those focused on regulatory circuits controlling the production of *S. aureus* virulence factors (43). We think that the results we report support the hypothesis that *sarA* is a valid target, in that they suggest that, even under circumstances in which *purR* production and/or function is reduced as a result of environmental pressures *in vivo*, inhibition of *sarA* would remain effective with respect to limiting the virulence of *S. aureus* in diverse forms of infection, including osteomyelitis.

MATERIALS AND METHODS

Ethics statement. All animal experiments were approved by the Institutional Animal Care and Use Committee of the University of Arkansas for Medical Sciences and were performed in compliance with NIH guidelines, the Animal Welfare Act, and U.S. federal law.

Bacterial strains and growth conditions. Bacterial strains used in this study are summarized in Table S3 in the supplemental material. The Tn-Seq library used in these studies was generated in the USA300 strain LAC and has been described previously (15). Mutants constructed during the course of the studies we report were generated in an erythromycin-sensitive derivative of LAC by Ø11-mediated transduction from existing JE2 mutants available in the Nebraska Transposon Mutant Library (44). Protease-deficient derivatives of LAC unable to produce aureolysin, ScpA, SspA, or SspB were generated as described previously (24, 28); *sarA* and/or *purR* mutations were then introduced into the protease-deficient strain by Ø11-mediated transduction. Strains were stored at -80°C in TSB containing 25% (vol/vol) glycerol. For each experiment, strains were recovered from storage by plating on tryptic soy agar with appropriate antibiotic selection. Antibiotics used were erythromycin (5 $\mu\text{g}/\text{ml}$), kanamycin (50 $\mu\text{g}/\text{ml}$), and neomycin (50 $\mu\text{g}/\text{ml}$). For phenotypic assays, all strains were grown at 37°C in TSB without antibiotics, with constant aeration.

Growth conditions for Tn-Seq comparisons. The Tn-Seq library was generated as described previously in a derivative of the USA300 strain LAC that had been cured of its erythromycin resistance plasmid, thus allowing for selection of transposon insertions (15). An aliquot of the library was thawed on ice and used to inoculate 500 ml of TSB containing erythromycin (5 $\mu\text{g}/\text{ml}$). This culture was grown to exponential phase (OD_{600} of 1) before cells were harvested and resuspended in TSB containing 25% (vol/vol) glycerol. Aliquots containing 1×10^9 CFU were then stored at -80°C .

Tn-Seq experiments in this study were conducted by thawing three 100- μl aliquots of the library and inoculating each as an independent biological replicate in 25 ml of biofilm medium (TSB supplemented with 0.5% glucose and 3.0% sodium chloride) containing 5 $\mu\text{g}/\text{ml}$ erythromycin. These cultures were incubated at 37°C with constant aeration and grown to exponential phase (OD_{600} of 1). A 8.0-ml aliquot of each replicate was removed and injected into individual chambers of a biofilm flow cell (described below). The remaining culture was allowed to grow to stationary phase (OD_{600} of ~ 10), and $\sim 5 \times 10^9$ CFU were harvested for genomic DNA (gDNA) extraction and sequencing as described below. Reads obtained from these stationary-phase planktonic cultures were used as the baseline comparator for Tn-Seq results observed in mature biofilms.

Biofilms were generated in disposable flow cells (IBI Scientific, Dubuque, IA) as described previously (27). Briefly, flow cells were precoated overnight at 4°C with 4 ml of 20% human plasma diluted in carbonate buffer (pH 9.6). A sterile reservoir of biofilm medium containing erythromycin (5 $\mu\text{g}/\text{ml}$) was connected to the inlet side of each flow cell, while the outlet side was connected to a waste reservoir. A total of 8.0 ml of biofilm medium containing 4×10^8 colony-forming units (CFU) was incubated at 37°C for 8 h without shaking to allow bacterial cells to adhere to the surface of the flow cells. The flow of sterile medium was then started at a rate of 0.5 ml/min and continued for 7 days, at which time bacterial cells were harvested and extracellular DNA was removed as described previously (45). Bacterial cells were then pelleted by centrifugation at 4,000 rpm for 10 min at 4°C , and gDNA was extracted and processed for sequencing as described below. The numbers of CFU following the 7-day incubation period were assessed and found to be comparable for the three flow cells, with an average colony count of 5×10^{10} CFU.

Tn-Seq library preparation. In all Tn-Seq experiments, gDNA was extracted using the NucleoBond HMW DNA kit (TaKaRa Bio USA, Inc., Mountain View, CA) according to the manufacturer's instructions

with the additional step of incubating the cells in 560 μ l Tris-EDTA (TE) (pH 8.0) containing lysostaphin (1 μ g/ μ l) prior to the enzymatic lysis step included as part of the standard kit protocol. The gDNA was then quantified, and 45 μ g from each sample was diluted in 150 μ l TE before shearing to a peak fragment size of \sim 250 bp using an ME220 focused-ultrasonicicator (Covaris, Woburn, MA). Next, 1 μ g of sheared gDNA was subjected to the NEBNext Ultra II DNA library preparation kit for Illumina (New England Biolabs, Ipswich, MA) protocol with key modifications to the PCR amplification step. Specifically, a nested PCR was carried out in which the first PCR was performed with the olj510 forward primer specific to the transposon (15) and the NEBNext indexed reverse primers obtained from NEBNext multiplex oligonucleotides for Illumina were used to amplify the transposon-gDNA junctions, to add a unique barcode to each sample, and to attach the p7 Illumina adaptor. The cycling conditions for this PCR were 98° C for 30 s, 98° C for 10 s, 65° C for 75 s for 25 cycles, and 65° C for 5 min. The second PCR was performed to enhance specificity for the transposon and to attach the p5 Illumina adaptor. Here, the olj511 forward primer specific to the inverted repeat region of the transposon (15) and the NEBNext indexed reverse primers were used with cycling conditions of 98° C for 30 s, 98° C for 10 s, 65° C for 75 s for 15 cycles, and 65° C for 5 min. The quality of the libraries was assessed via the TapeStation (Agilent, Santa Clara, CA) and quantitative real-time PCR using the olj512 primer specific to the transposon terminal inverted repeat of reference 15. The validated libraries were then sequenced using the custom sequencing primer olj512 on an Illumina HiSeq 2500 high-output v4 (single-end 100-bp reads) at the Tufts University Core Facility.

Tn-Seq analysis. The *S. aureus* USA300 LAC genome of the library parent strain was used as the reference for all Tn-Seq analyses in this study. We previously sequenced this strain and assembled a complete genome, which has since been deposited in GenBank (GenBank accession numbers [CP055225](#) and [CP055226](#)). In-house scripts were used for the analyses. Briefly, BWA-MEM was used to align reads to the reference genome (46). Alignments were then further processed using SAMtools and BEDtools to retrieve, to count, and to sum all reads aligned to TA sites (47, 48). Next, the mean counts per gene were normalized by the TTR method in the Transit package, and genes with significant changes in the number of transposon insertions between the comparator planktonic cultures and the mature biofilms were distilled by the ZINB method (49). Genes with a \log_2 fold change of ± 1.0 and a *P* value of >0.05 were considered significant and are listed in Table S1. A positive \log_2 fold change value in Table S1 indicates increased insertions in biofilm, compared to planktonic cultures, i.e., increased fitness in biofilm. Negative values indicate reduced fitness in biofilm. Data were visualized using the R package ggplot2 (50).

Clumping assays. This assay was conducted as described previously (2). Briefly, overnight cultures were diluted to an OD_{600} of 0.03 in 2 ml of either TSB or TSB containing 10% (vol/vol) horse serum (TSB-S). Cultures were incubated for 3.5 h at 37° C with shaking and constant aeration. The culture was then placed upright and allowed to stand statically for 5 min, to allow cellular clumps to settle. The absorbance of the culture was measured based on a sample taken from the upper portion of the culture. Results are reported based on three biological replicates, each of which included three experimental replicates.

Static biofilm assay. Biofilm formation was assessed using a microtiter plate assay using four different assay conditions (27). The differences were based on the composition of the medium and whether the wells of the microtiter plate were first coated with human plasma proteins. Specifically, each strain was grown in TSB supplemented with 0.5% glucose with or without supplementation with 0.3% NaCl. Strains were grown overnight in each of these two medium formulations and standardized to an OD_{600} of 0.05 in fresh medium corresponding to the same medium used for overnight growth. Cultures were then split and added to the wells of the microtiter plate with or without coating overnight at 4° C with 100 μ l of 20% human plasma diluted in carbonate buffer (pH 9.6). Biofilm assays were performed under each of the four resulting conditions using previously described methods (27). Results are based on three biological replicates, each of which included six experimental replicates.

CM preparation. Overnight cultures grown in TSB without antibiotic selection were standardized to an OD_{600} of 0.05 in fresh TSB and grown to an OD_{600} of 1.0 (mid-exponential phase) or overnight. Overnight cultures were standardized to an OD_{600} of 10. At each time point, cultures were clarified by centrifugation and the supernatant was sterilized by filtration. The resulting CM was used immediately or stored at -20° C for Western blotting with anti-alpha toxin and anti-protein A antibodies as described previously (9).

Whole-cell lysate preparation. SarA Western blots were performed with an anti-SarA antibody and whole-cell lysates prepared as described previously (31). Briefly, strains were cultured overnight at 37° C in TSB with constant shaking. Bacterial cells from a volume of each culture calculated to obtain an equivalent number of cells were harvested by centrifugation, washed with sterile phosphate-buffered saline (PBS), and resuspended in 750 μ l of TEG buffer (25 mM Tris-HCl [pH 8.0], 25 mM EGTA). Cell suspensions were stored at -20° C until all samples had been collected, at which point samples were thawed on ice, transferred to FastPrep lysing matrix B tubes, and lysed in a FastPrep-24 benchtop homogenizer (MP Biomedicals) using two 40-s intervals at a rate of 6.0 m/s, interrupted by a 5-min interval during which the homogenates were chilled on ice. After centrifugation at 15,000 $\times g$ for 10 min at 4° C, supernatants were harvested and stored at -80° C.

Extracellular protease activity. Overall extracellular protease activity was assessed using CM and the EnzCheck FRET-based gelatinase/collagenase assay (Thermo Fisher Scientific, Waltham, MA) according to the manufacturer's protocol.

Murine model of osteomyelitis. The relative capacity of each strain to cause osteomyelitis was assessed using our murine model as described previously (9, 29). Briefly, 6- to 8-week-old C57BL/6 mice

were anesthetized, and an incision was made in the right hind limb to expose the femur. A unicortical defect was created in the central region of the right femur, and $2\ \mu\text{l}$ of a bacterial suspension containing 1×10^6 CFU harvested from exponential-phase cultures (OD_{600} of 1.0) was introduced directly into the intramedullary canal. The wound was then closed and the infection was allowed to develop for 14 days, at which time the mice were humanely euthanized and the infected femurs were harvested for microcomputed tomography (μCT) analysis or for quantitation of bacterial burdens.

Microcomputed tomography. Image acquisition and analysis were performed according to previously published protocols (9, 29). Briefly, imaging was performed with the SkyScan 1174 X-ray microtomograph (Bruker, Kontich, Belgium) using an isotropic voxel size of $6.7\ \mu\text{m}$, an X-ray voltage of 50 kV (800 μA), and a 0.25-mm aluminum filter. Reconstruction was carried out using the SkyScan NRecon software, and the reconstructed cross-sectional slices were processed as described previously, using the SkyScan CT-Analyzer software. Using the bone-including binarized images, a semiautomated protocol was run to delineate regions of interest (ROIs) in which the reactive new bone (callus) was isolated from the cortical bone. The resulting images were loaded as ROIs and corrected by drawing inclusive or exclusive contours on the periosteal surface to keep only and strictly the cortical bone. Using these defined ROIs, the volume of cortical bone was calculated; the amount of cortical bone destruction was estimated by subtracting the value obtained from each bone from the average obtained from sham-operated bones inoculated with PBS. New bone formation was quantified by using the subtractive ROI function on the previously delineated cortical bone-including ROI images and calculating the bone volume included in the newly defined ROIs. Statistical analysis of data from each experimental group was performed by one-way analysis of variance (ANOVA). Contrasts were defined to address comparisons of interest, which included assessing the effects among isogenic mutants (*LAC*, *sarA*, *purR*, and *sarApurR*) and between protease-deficient and parent strains. Unadjusted *P* values were calculated using permutation tests, and multiplicity adjustments were performed using the Benjamini-Hochberg method, commonly known as the false discovery rate (FDR) adjustment. *P* values of ≤ 0.05 were considered statistically significant.

Bacterial burdens in the femur. Bacterial loads in each femur were determined as reported previously, with minor modifications (9). Briefly, femurs were separated from surrounding soft tissue and homogenized using the Bullet Blender 5 Gold tissue homogenizer (Next Advance, Troy, NY). The 5-ml Navy kit from the same manufacturer was filled with 2 ml sterile PBS prior to placement of the intact femur in the tube. The homogenizer was then run for 10 min at speed of 20 rpm. Subsequently, homogenates were vortex-mixed, serially diluted, and plated on TSB solidified with 1.5% agar. Statistical differences between groups were assessed after logarithmic transformation of CFU data, as described in the previous section.

SUPPLEMENTAL MATERIAL

Supplemental material is available online only.

SUPPLEMENTAL FILE 1, PDF file, 0.04 MB.

SUPPLEMENTAL FILE 1, XLSX file, 0.01 MB.

SUPPLEMENTAL FILE 2, XLSX file, 0.01 MB.

SUPPLEMENTAL FILE 3, XLSX file, 0.01 MB.

ACKNOWLEDGMENTS

We thank Anthony R. Richardson of the University of Pittsburgh for sharing the TnSeq library used in this study and for his comments on the manuscript.

D.A. is supported by National Science Foundation award OIA-1946391. M.S.S. is supported by NIH grant R01-AI119380, the Arkansas Research Alliance, and a generous gift from the Texas Hip and Knee Society. We acknowledge the Tufts University genomics core and the University of Arkansas for Medical Sciences Sequencing Core Facility, supported in part by the Center for Microbial Pathogenesis and Host Inflammatory Responses grant P20GM103625 through the NIH National Institute of General Medical Sciences Centers of Biomedical Research Excellence.

The content is solely the responsibility of the authors and does not necessarily represent the official views of the NIH.

REFERENCES

1. Sause WE, Balasubramanian D, Irnov I, Copin R, Sullivan MJ, Sommerfield A, Chan R, Dhabaria A, Askenazi M, Ueberheide B, Shopsin B, van Bakel H, Torres VJ. 2019. The purine biosynthesis regulator PurR moonlights as a virulence regulator in *Staphylococcus aureus*. *Proc Natl Acad Sci U S A* 116:13563–13572. <https://doi.org/10.1073/pnas.1904280116>.
2. Goncheva MI, Flannagan RS, Sterling BE, Laakso HA, Friedrich NC, Kaiser JC, Watson DW, Wilson CH, Sheldon JR, McGavin MJ, Kiser PK, Heinrichs DE. 2019. Stress-induced inactivation of the *Staphylococcus aureus* purine biosynthesis repressor leads to hypervirulence. *Nat Commun* 10:775. <https://doi.org/10.1038/s41467-019-108724-x>.
3. Goncheva MI, Flannagan RS, Heinrichs DE. 2020. *De novo* purine biosynthesis is required for intracellular growth of *Staphylococcus aureus* and for the hypervirulence phenotype of a *purR* mutant. *Infect Immun* 88: e00104-20. <https://doi.org/10.1128/IAI.00104-20>.
4. McLean K, Holmes EA, Penewit K, Lee DK, Hardy SR, Ren M, Krist MP, Huang K, Waalkes A, Salipante SJ. 2019. Artificial selection for pathogenicity mutations in *Staphylococcus aureus* identifies novel factors relevant to

chronic infection. *Infect Immun* 87:e00884-18. <https://doi.org/10.1128/IAI.00884-18>.

5. Cheung AL, Ying P. 1994. Regulation of alpha- and beta-hemolysins by the *sar* locus of *Staphylococcus aureus*. *J Bacteriol* 176:580–585. <https://doi.org/10.1128/jb.176.3.580-585.1994>.
6. Chien Y, Manna AC, Cheung AL. 1998. SarA level is a determinant of *agr* activation in *Staphylococcus aureus*. *Mol Microbiol* 30:991–1001. <https://doi.org/10.1046/j.1365-2958.1998.01126.x>.
7. Byrum SD, Loughran AJ, Beenken KE, Orr LM, Storey AJ, Mackintosh SG, Edmondson RD, Tackett AJ, Smeltzer MS. 2018. Label-free proteomic approach to characterize protease-dependent and -independent effects of *sarA* inactivation on the *Staphylococcus aureus* exoproteome. *J Proteome Res* 17:3384–3395. <https://doi.org/10.1021/acs.jproteome.8b00288>.
8. Kolar SL, Ibarra JA, Rivera FE, Mootz JM, Davenport JE, Stevens SM, Horswill AR, Shaw LN. 2013. Extracellular proteases are key mediators of *Staphylococcus aureus* virulence via the global modulation of virulence-determinant stability. *Microbiologyopen* 2:18–34. <https://doi.org/10.1002/mbo3.55>.
9. Ramirez AM, Byrum SD, Beenken KE, Washam C, Edmondson RD, Mackintosh SG, Spencer HJ, Tackett AJ, Smeltzer MS. 2020. Exploiting correlations between protein abundance and the functional status of *saeRS* and *sarA* to identify virulence factors of potential importance in the pathogenesis of *Staphylococcus aureus* osteomyelitis. *ACS Infect Dis* 6:237–249. <https://doi.org/10.1021/acsinfecdis.9b00291>.
10. Zielinska AK, Beenken KE, Joo HS, Mrak LN, Griffin LM, Luong TT, Lee CY, Otto M, Shaw LN, Smeltzer MS. 2011. Defining the strain-dependent impact of the staphylococcal accessory regulator (*sarA*) on the alpha-toxin phenotype of *Staphylococcus aureus*. *J Bacteriol* 193:2948–2958. <https://doi.org/10.1128/JB.01517-10>.
11. Zielinska AK, Beenken KE, Mrak LN, Spencer HJ, Post GR, Skinner RA, Tackett AJ, Horswill AR, Smeltzer MS. 2012. *sarA*-mediated repression of protease production plays a key role in the pathogenesis of *Staphylococcus aureus* USA300 isolates. *Mol Microbiol* 86:1183–1196. <https://doi.org/10.1111/mmi.12048>.
12. Mauffrey C, Herbert B, Young H, Wilson ML, Hake M, Stahel PF. 2016. The role of biofilm on orthopaedic implants: the Holy Grail of post-traumatic infection management? *Eur J Trauma Emerg Surg* 42:411–416. <https://doi.org/10.1007/s00068-016-0694-1>.
13. Zimmerli W, Sendi P. 2017. Orthopaedic biofilm infections. *APMIS* 125:353–364. <https://doi.org/10.1111/apm.12687>.
14. van Opijnen T, Bodi KL, Camilli A. 2009. Tn-seq: high-throughput parallel sequencing for fitness and genetic interaction studies in microorganisms. *Nat Methods* 6:767–772. <https://doi.org/10.1038/nmeth.1377>.
15. Grosser MR, Paluscio E, Thurlow LR, Dillon MM, Cooper VS, Kawula TH, Richardson AR. 2018. Genetic requirements for *Staphylococcus aureus* nitric oxide resistance and virulence. *PLoS Pathog* 14:e1006907. <https://doi.org/10.1371/journal.ppat.1006907>.
16. Crosby HA, Schlievert PM, Merriman JA, King JM, Salgado-Pabon W, Horswill AR. 2016. The *Staphylococcus aureus* global regulator MgrA modulates clumping and virulence by controlling surface protein expression. *PLoS Pathog* 12:e1005604. <https://doi.org/10.1371/journal.ppat.1005604>.
17. Trotonda MP, Tamber S, Memmi G, Cheung AL. 2008. MgrA represses biofilm formation in *Staphylococcus aureus*. *Infect Immun* 76:5645–5654. <https://doi.org/10.1128/IAI.00735-08>.
18. Jefferson KK, Pier DB, Goldmann DA, Pier GB. 2004. The teicoplanin-associated locus regulator (TcaR) and the intercellular adhesin locus regulator (IcaR) are transcriptional inhibitors of the *ica* locus in *Staphylococcus aureus*. *J Bacteriol* 186:2449–2456. <https://doi.org/10.1128/jb.186.8.2449-2456.2004>.
19. Paharik AE, Horswill AR. 2016. The staphylococcal biofilm: adhesins, regulation, and host response. *Microbiol Spectr* 4:VMBF-0022-2015. <https://doi.org/10.1128/microbiolspec.VMBF-0022-2015>.
20. Lauderdale KJ, Boles BR, Cheung AL, Horswill AR. 2009. Interconnections between sigma B, *agr*, and proteolytic activity in *Staphylococcus aureus* biofilm maturation. *Infect Immun* 77:1623–1635. <https://doi.org/10.1128/IAI.01036-08>.
21. Wilde AD, Snyder DJ, Putnam NE, Valentino MD, Hammer ND, Lonergan ZR, Hinger SA, Aysanoa EE, Blanchard C, Dunman PM, Wasserman GA, Chen J, Shopsin B, Gilmore MS, Skaar EP, Cassat JE. 2015. Bacterial hypoxic responses revealed as critical determinants of the host-pathogen outcome by TnSeq analysis of *Staphylococcus aureus* invasive infection. *PLoS Pathog* 11:e1005341. <https://doi.org/10.1371/journal.ppat.1005341>.
22. Atwood DN, Loughran AJ, Courtney AP, Anthony AC, Meeker DG, Spencer HJ, Gupta RK, Lee CY, Beenken KE, Smeltzer MS. 2015. Comparative impact of diverse regulatory loci on *Staphylococcus aureus* biofilm formation. *Microbiologyopen* 4:436–451. <https://doi.org/10.1002/mbo3.250>.
23. Atwood DN, Beenken KE, Lantz TL, Meeker DG, Lynn WB, Mills WB, Spencer HJ, Smeltzer MS. 2016. Regulatory mutations impacting antibiotic susceptibility in an established *Staphylococcus aureus* biofilm. *Antimicrob Agents Chemother* 60:1826–1829. <https://doi.org/10.1128/AAC.02750-15>.
24. Beenken KE, Mrak LN, Zielinska AK, Atwood DN, Loughran AJ, Griffin LM, Matthews KA, Anthony AM, Spencer HJ, Skinner RA, Post GR, Lee CY, Smeltzer MS. 2014. Impact of the functional status of *saeRS* on *in vivo* phenotypes of *Staphylococcus aureus* *sarA* mutants. *Mol Microbiol* 92:1299–1312. <https://doi.org/10.1111/mmi.12629>.
25. Tsang LH, Cassat JE, Shaw LN, Beenken KE, Smeltzer MS. 2008. Factors contributing to the biofilm-deficient phenotype of *Staphylococcus aureus* *sarA* mutants. *PLoS One* 3:e3361. <https://doi.org/10.1371/journal.pone.0003361>.
26. Mrak LN, Zielinska AK, Beenken KE, Mrak IN, Atwood DN, Griffin LM, Lee CY, Smeltzer MS. 2012. *saeRS* and *sarA* act synergistically to repress protease production and promote biofilm formation in *Staphylococcus aureus*. *PLoS One* 7:e38453. <https://doi.org/10.1371/journal.pone.0038453>.
27. Beenken KE, Blevins JS, Smeltzer MS. 2003. Mutation of *sarA* in *Staphylococcus aureus* limits biofilm formation. *Infect Immun* 71:4206–4211. <https://doi.org/10.1128/IAI.71.7.4206-4211.2003>.
28. Loughran AJ, Atwood DN, Anthony AC, Harik NS, Spencer HJ, Beenken KE, Smeltzer MS. 2014. Impact of individual extracellular proteases on *Staphylococcus aureus* biofilm formation in diverse clinical isolates and their isogenic *sarA* mutants. *Microbiologyopen* 3:897–909. <https://doi.org/10.1002/mbo3.214>.
29. Loughran AJ, Gaddy D, Beenken KE, Meeker DG, Morello R, Zhao H, Byrum SD, Tackett AJ, Cassat JE, Smeltzer MS. 2016. Impact of *sarA* and phenol-soluble modulins on the pathogenesis of osteomyelitis in diverse clinical isolates of *Staphylococcus aureus*. *Infect Immun* 84:2586–2594. <https://doi.org/10.1128/IAI.00152-16>.
30. Rom JS, Atwood DN, Beenken KE, Meeker DG, Loughran AJ, Spencer HJ, Lantz TL, Smeltzer MS. 2017. Impact of *Staphylococcus aureus* regulatory mutations that modulate biofilm formation in the USA300 strain LAC on virulence in a murine bacteremia model. *Virulence* 8:1776–1790. <https://doi.org/10.1080/21505594.2017.1373926>.
31. Rom JS, Ramirez AM, Beenken KE, Sahukhal GS, Elasri MO, Smeltzer MS. 2019. The impacts of *msaABC* on *sarA*-associated phenotypes are different in divergent clinical isolates of *Staphylococcus aureus*. *Infect Immun* 88:e00530-19. <https://doi.org/10.1128/IAI.00530-19>.
32. Claro T, Widaa A, O'Seaghda M, Mjavilovic H, Foster TJ, O'Brien FJ, Kerrigan SW. 2011. *Staphylococcus aureus* protein A binds to osteoblasts and triggers signals that weaken bone in osteomyelitis. *PLoS One* 6:e18748. <https://doi.org/10.1371/journal.pone.0018748>.
33. Jin T, Zhu YL, Li J, Shi J, He XQ, Ding J, Xu YQ. 2013. Staphylococcal protein A, Panton-Valentine leukocidin and coagulase aggravate the bone loss and bone destruction in osteomyelitis. *Cell Physiol Biochem* 32:322–333. <https://doi.org/10.1159/000354440>.
34. Mendoza Bertelli A, Delpino MV, Lattar S, Giai C, Llana MN, Sanjuan N, Cassat JE, Sordelli D, Gomez MI. 2016. *Staphylococcus aureus* protein A enhances osteoclastogenesis via TNFR1 and EGFR signaling. *Biochim Biophys Acta* 1862:1975–1983. <https://doi.org/10.1016/j.bbadi.2016.07.016>.
35. Widaa A, Claro T, Foster TJ, O'Brien FJ, Kerrigan SW. 2012. *Staphylococcus aureus* protein A plays a critical role in mediating bone destruction and bone loss in osteomyelitis. *PLoS One* 7:e40586. <https://doi.org/10.1371/journal.pone.0040586>.
36. Potter AD, Butrico CE, Ford CA, Curry JM, Trenary IA, Tummarakota SS, Hendrix AS, Young JD, Cassat JE. 2020. Host nutrient milieu drives an essential role for aspartate biosynthesis during invasive *Staphylococcus aureus* infection. *Proc Natl Acad Sci U S A* 117:12394–12401. <https://doi.org/10.1073/pnas.1922211117>.
37. Ahmed S, Meghji S, Williams RJ, Henderson B, Brock JH, Nair SP. 2001. *Staphylococcus aureus* fibronectin binding proteins are essential for internalization by osteoblasts but do not account for differences in intracellular levels of bacteria. *Infect Immun* 69:2872–2877. <https://doi.org/10.1128/IAI.69.5.2872-2877.2001>.
38. Horn J, Stelzner K, Rudel T, Fraunholz M. 2018. Inside job: *Staphylococcus aureus* host-pathogen interactions. *Int J Med Microbiol* 308:607–624. <https://doi.org/10.1016/j.ijmm.2017.11.009>.
39. McCourt J, O'Halloran DP, McCarthy H, O'Gara JP, Geoghegan JA. 2014. Fibronectin-binding proteins are required for biofilm formation by

community-associated methicillin-resistant *Staphylococcus aureus* strain LAC. FEMS Microbiol Lett 353:157–164. <https://doi.org/10.1111/1574-6968.12424>.

40. Atwood DN, Beenken KE, Loughran AJ, Meeker DG, Lantz TL, Graham JW, Spencer HJ, Smeltzer MS. 2016. XerC contributes to diverse forms of *Staphylococcus aureus* infection via *agr*-dependent and *agr*-independent pathways. Infect Immun 84:1214–1225. <https://doi.org/10.1128/IAI.01462-15>.

41. Lehman MK, Nuxoll AS, Yamada KJ, Kielian T, Carson SD, Fey PD. 2019. Protease-mediated growth of *Staphylococcus aureus* on host proteins is *opp3* dependent. mBio 10:e02553-18. <https://doi.org/10.1128/mBio.02553-18>.

42. Pietrocola G, Nobile G, Rindi S, Speziale P. 2017. *Staphylococcus aureus* manipulates innate immunity through own and host-expressed proteases. Front Cell Infect Microbiol 7:166. <https://doi.org/10.3389/fcimb.2017.00166>.

43. Kane TL, Carothers KE, Lee SW. 2018. Virulence factor targeting of the bacterial pathogen *Staphylococcus aureus* for vaccine and therapeutics. Curr Drug Targets 19:111–127. <https://doi.org/10.2174/1389450117666161128123536>.

44. Fey PD, Endres JL, Yajjala VK, Widholm TJ, Boissy RJ, Bose JL, Bayles KW. 2013. A genetic resource for rapid and comprehensive phenotype screening of nonessential *Staphylococcus aureus* genes. mBio 4:e00537-12. <https://doi.org/10.1128/mBio.00537-12>.

45. DeFrancesco AS, Masloboeva N, Syed AK, DeLoughery A, Bradshaw N, Li GW, Gilmore MS, Walker S, Losick R. 2017. Genome-wide screen for genes involved in eDNA release during biofilm formation by *Staphylococcus aureus*. Proc Natl Acad Sci U S A 114:E5969–E5978. <https://doi.org/10.1073/pnas.1704544114>.

46. Li H. 2013. Aligning sequence reads, clone sequences and assembly contigs with BWA-MEM. arXiv 13033997.

47. Li H. 2011. A statistical framework for SNP calling, mutation discovery, association mapping and population genetical parameter estimation from sequencing data. Bioinformatics 27:2987–2993. <https://doi.org/10.1093/bioinformatics/btr509>.

48. Barnett DW, Garrison EK, Quinlan AR, Stromberg MP, Marth GT. 2011. BamTools: a C++ API and toolkit for analyzing and managing BAM files. Bioinformatics 27:1691–1692. <https://doi.org/10.1093/bioinformatics/btr174>.

49. Subramaniyam S, DeJesus MA, Zaveri A, Smith CM, Baker RE, Ehrt S, Schnappinger D, Sasetti CM, Ioerger TR. 2019. Statistical analysis of variability in TnSeq data across conditions using zero-inflated negative binomial regression. BMC Bioinformatics 20:603. <https://doi.org/10.1186/s12859-019-3156-z>.

50. Wickham H. 2016. ggplot2: elegant graphics for data analysis. Springer-Verlag, New York, NY.